

## NUMERICAL SIMULATION OF A FIBER LASER BENDING SENSITIVITY

S. MICLOS<sup>1</sup>, D. SAVASTRU<sup>1</sup>, I. LANCRANJAN<sup>2</sup>

<sup>1</sup>National Institute of R&D for Optoelectronics - INOE 2000, 409 Atomistilor Str., POB MG-5,  
RO-077125 Magurele, Ilfov, Romania, E-mail: miclos@inoe.inoe.ro; dsavas@inoe.inoe.ro

<sup>2</sup>Advanced Study Center–National Institute of Aerospace Research “Elie Carafoli”, 220 Iuliu Maniu  
Boulevard, RO-061126, Bucharest, Romania, E-mail: j\_j\_f\_l@yahoo.com

(Received May 17, 2010)

*Abstract.* Numerical simulation analysis of fiber optic bending sensitivity aiming to improve fiber lasers design is developed, analyzing both the transition loss, associated with abrupt curvature change at the beginning and the end of a bend, and pure bending loss associated with the loss from the constant curvature bending in between.

*Key words:* fiber laser, eigenmodes, laser field, numerical simulation, COMSOL.

### 1. INTRODUCTION

Fiber lasers are attractive devices for an increasingly number of applications in the material processing, laboratory research and telecommunication areas due to their inherit fiber compatibility, stable single longitudinal mode, and single polarization operation. They are inherently fiber compatible. In addition, they have low phase noise as well as low relative intensity noise (RIN). A number of different active dopants, such as erbium, ytterbium, neodymium, and thulium, can be used in order to cover different windows of the optical spectrum and offer extended coverage.

An accurate model of these types of lasers is very desirable since the simulations can reduce the design and development time and cost significantly. A model can also help to improve the physical insight on the device or system under investigation by allowing one to carry out calculations and hypothetical experiments, which in many cases can be extremely difficult in laboratory conditions. The full description of a fiber laser considering the phenomena developed in the active medium would include many linear and nonlinear equations. The second difficulty is the measurement of the actual values of the

parameters and coefficients that appear in these equations [1–7]. The solution of the ideal model with all the possible transitions is impractical. Therefore, in practice, the solution of complex active medium equations, whether it is an analytical or numerical solution, inevitably requires simplifications and approximations. Ignoring some of less significant transitions in the active medium, a set of equations reported to be successfully modeling the amplifier regime [1] and purely theoretical works investigating the implications of these simplifications have been reported [2, 3].

An important part of such an accurate numerical simulation model will be dedicated to the investigation of pumping and output beams propagation along the optic fiber defining the active medium volume. One reason for which fiber laser are preferred against other laser types consists in their high ratio output power versus pumping. A small volume of fiber laser active medium can be obtained by using coils of doped optic fiber. Bending loss of laser power induced into the optic fiber become of importance in order to achieve a proper simulation and design of fiber lasers. In this paper preliminary results obtained in investigating the laser field propagation through non-deformed and deformed optic fiber are presented. Symmetrical deformation of optic fiber is considered in order to simulate its bending at microscopic scale (micro-bending).

## 2. THEORY

A mode propagating on a straight fiber or waveguide fabricated from non-absorbing, non-scattering materials will in principle propagate indefinitely without any loss of power. However, if a bend is introduced, the translational invariance is broken and power is lost from the mode as it propagates into, along and out of the bend. This applies to the fundamental mode in the case of single-mode fibers and waveguides and to all bound modes in the case of bent multimode fibers or waveguides.

Two types of optic fiber bend losses can be considered [8, 9]:

- transition loss is associated with the abrupt or rapid change in curvature at the beginning and the end of a bend;
- pure bend loss is associated with the loss from the bend of constant curvature in between the optic fiber.

The transition loss can be described by an abrupt change in the curvature  $k$  from the straight waveguide ( $k \sim 0$ ) to that of the bent waveguide of constant radius  $R_b$  ( $k = 1/R_b$ ). The fundamental-mode field is shifted slightly outwards in the plane of the bend, thereby causing a miss-match with the field of the straight waveguide, as presented in Fig. 1. The fractional loss in fundamental-mode power,  $\delta P/P$ , can be calculated from the overlap integral between the fields. Within the Gaussian approximation to the fundamental mode field and assuming that the spot size  $s$  and core radius or half-width  $r$  are approximately equal, this gives Eq. (1):

$$\frac{\delta P}{P} \approx \frac{1}{16} \frac{V^4}{\Delta^2} \frac{\rho^2}{R_b^2}, \quad (1)$$

where  $V$  is the fiber or waveguide parameter and  $\Delta$  is the relative index difference.

Minimizing transition loss can be achieved by considering a number of techniques for significantly reducing transition loss. In the case of planar waveguides it is often possible to fabricate the bend so that there is an abrupt offset between the cores of the straight and bent waveguides in the plane of the bend. In Fig. 1 this can be seen as being equivalent to displacing the bent core downwards so that the two fundamental-mode fields overlap. Alternatively, if a gradual increase in curvature is introduced between the straight and uniformly bent sections, the fundamental field of the straight waveguide will evolve approximately adiabatically into the offset field of the uniformly bent section.

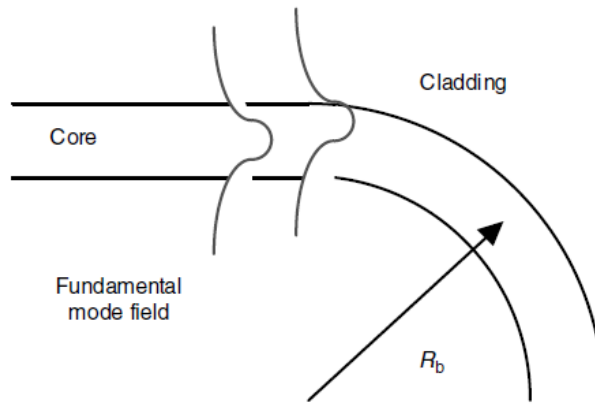


Fig. 1 – Outward shift in the fundamental-mode electric field on entering a bend.

The pure bent loss is defined by the fundamental mode continuously optical power loses when propagating along the curved path of the core of constant radius  $R_b$ . It is assumed that the cladding is essentially unbounded and not affected by the fiber optic bend, keeping a constant clad refractive index value,  $n_{cl}$ . The radiation loss increases rapidly with decreasing bend radius and occurs predominantly in the plane of the bend; in any other plane the effective bend radius is larger and hence the loss is very much reduced, as presented in Fig. 1. It has to be observed that the phase velocity anywhere on the modal phase front rotating around the bend cannot exceed the speed of light in the cladding. Hence, beyond radius  $R_{rad}$  the modal field must necessarily radiate into the cladding, the radiation being emitted tangentially. The interface between the guided portion of the modal field around the bend and the radiated portion at  $R_{rad}$  is known as the radiation caustic, and is the apparent

origin of radiation. Between the core and the radiation caustic, the modal field is evanescent and decreases approximately exponentially with increasing radial distance from C. As the bend radius increases, the radiation caustic moves farther into the cladding, and the level of radiated power decreases.  $R_{rad}$  can be defined by the Eq. (2):

$$R_{rad} = \frac{c}{\Omega n_{cl}}. \quad (2)$$

In investigating fiber optic bend losses and important issue has to be considered, namely the radiation caustic. It refers to the fact that phase velocity anywhere on the modal phase front rotating around the bend cannot exceed the speed of light in the cladding. Hence, beyond radius  $R_{rad}$  the modal field must necessarily radiate into the cladding, the radiation being emitted tangentially. The interface between the guided portion of the modal field around the bend and the radiated portion at  $R_{rad}$  is known as the radiation caustic, and is the apparent origin of radiation.

Between the core and the radiation caustic, the modal field is evanescent and decreases approximately exponentially with increasing radial distance from C. As the bend radius increases, the radiation caustic moves farther into the cladding, and the level of radiated power decreases. Conversely, as the bend radius decreases, the radiation caustic moves closer to the core and the radiation loss increases. In practical fibers, the radiated power from the bend is either absorbed by the acrylic coating surrounding the outside of the cladding or propagates through the coating into free space.

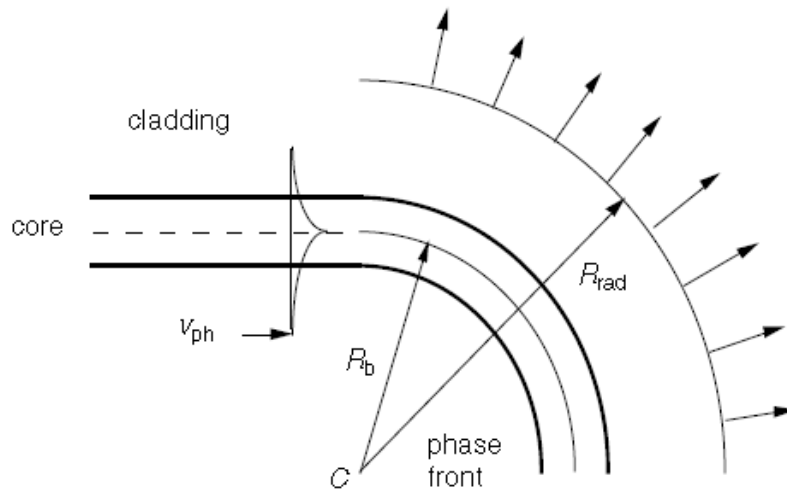


Fig. 2 – Schematic of the bending effect of a fiber optic.

Analytically the mode attenuation can be expressed as a function of  $z$ , where  $z$  is the distance from the beginning of the bend relative to the fiber axis. The total fundamental mode power  $P(z)$  attenuates according to Eq. (3),

$$P(z) = P(0)e^{-\gamma z}, \quad (3)$$

where  $P(0)$  is the total fundamental mode power entering the bend and  $\gamma$  is the power attenuation coefficient. In decibels, this relationship is equivalent to Eq. (4)

$$\text{dB} = 10 \lg \left( \frac{P(z)}{P(0)} \right) = 10 \lg \left( e^{-\gamma z} \right) = 20 \lg e \gamma z. \quad (4)$$

Eq. (4) indicates that the loss of power per unit length of bent fibre is  $8.686\gamma$  dB.

The present theoretical analysis is developed by considering optic fibers with step profile of the refractive index. In terms of the core and cladding modal parameters  $U$  and  $W$ , respectively, relative index difference  $\Delta$ , core radius  $r$ , fibre parameter  $V$  and the bend radius  $R_b$ , an approximate expression for  $\gamma$  for the fundamental mode of a step-profile fibre has the form [4]:

$$\gamma = \left( \frac{\pi \rho}{R_b} \right)^{1/2} \frac{V^2 W^{1/2}}{2 \rho U^2} e^{-\frac{4}{3} \frac{\Delta R_b W^3}{\rho V^2}}, \quad (5)$$

where  $R_b$  is necessarily large compared to  $r$  because it is not possible to bend a fibre into a radius much below 1 cm without breakage. The pure bend loss coefficient is most sensitive to the expression inside the exponent because  $R_b$  and  $r$ . Loss decreases very rapidly with increasing values of  $R_b$  or  $\Delta$  or  $V$  (since  $W$  also increases with  $V$ ), and becomes arbitrarily small as  $R_b \rightarrow \infty$ .

### 3. RESULTS AND DISCUSSION

The numerical simulation of the laser intensity distribution across the transverse section of the optic fiber is performed using COMSOL Multiphysics. The option **2D** was used for the **Space Dimension**. Then the **RF Module**  $\rightarrow$  **Perpendicular Waves**  $\rightarrow$  **Hybrid-Mode Waves**  $\rightarrow$  **Mode analysis options** was used. The geometry of the transverse optic fibre cross section was developed considering realistic parameters. Elliptical deformation of the optical fibre was considered in order to resemble the bend.

Only singlemode optical fiber was analyzed. The developed geometry of the studied optical fibre is considering the following refractive index values:

$n_{cl} = 1.4378$  – for the clad with an external diameter of 80  $\mu\text{m}$ ;

$n_{co} = 1.4457$  – for the core with a diameter of 10  $\mu\text{m}$ .

Numerical simulations were performed for optic fiber with and without doping with erbium ions ( $\text{Er}^{3+}$ ). No significant differences were observed for doped or undoped optic fibers. The numerical simulations were performed using  $1.550\ \mu\text{m}$  as the laser wavelength.

The procedure tried during numerical simulation consists in considering the laser beam propagation along the bending such as the optical fiber appears as of an elliptical cross section. The deformation was considered by imposing a mechanical stress/pressure on the external surface of the plastic protection layer deposited on the glass clad. The deformation is expressed in  $\mu\text{m}$ . The deformed dimensions of the glass clad and core (the ellipse axes) are calculated as the density is constant. The maximum value of the considered plastic layer deformation (denoted as strain) was of  $20\ \mu\text{m}$ .

In Figs. 3 and 4 the results obtained by numerical simulations in the case of non-deformed optic fiber are presented. The mesh grid has a number of 4,320 elements, meaning that the transverse linear dimension of such mesh element ( $\sim 0.015\ \mu\text{m}$ ) is far less than the considered laser field propagation wavelength. The basic hypothesis of electromagnetic field diffraction, hypothesis on which the used software was developed is fulfilled. In Fig. 3 the numerical simulated time averaged laser power flow across the transverse section of a singlemode optical fiber with a core of  $10\ \mu\text{m}$  diameter and a clad of an overall  $80\ \mu\text{m}$  diameter is presented. In Fig. 4 the numerical simulated time averaged laser electric field distribution into the transverse section of a mono-mode optical fiber with a core of  $10\ \mu\text{m}$  diameter and a clad of an overall  $80\ \mu\text{m}$  diameter is presented.

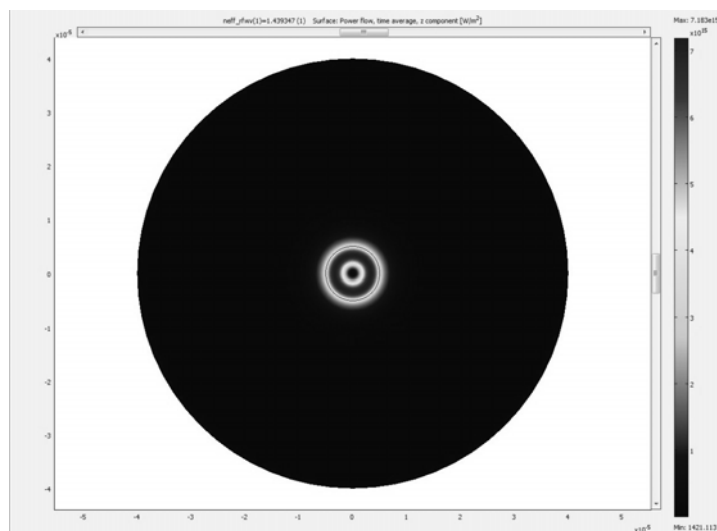


Fig. 3 – The numerical simulated time averaged laser power flow across the transverse section of a singlemode optical fiber with a core of  $10\ \mu\text{m}$  diameter and a cladding of an  $80\ \mu\text{m}$  overall diameter.

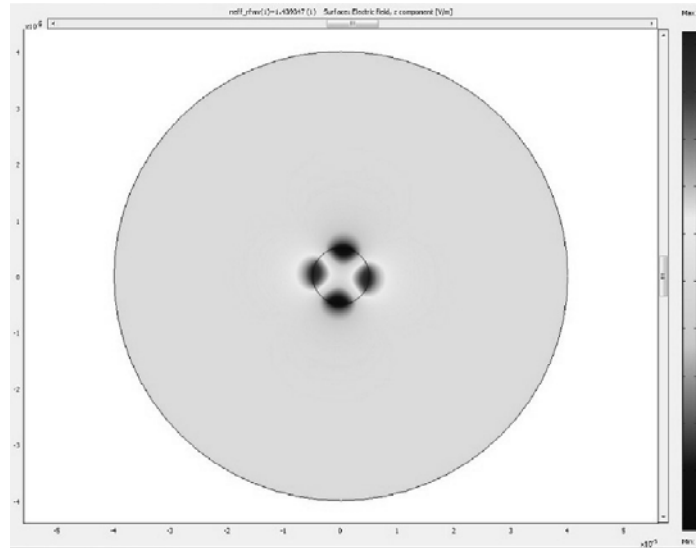


Fig. 4 – The numerical simulated time averaged laser electric field distribution into the transverse section of a singlemode optical fiber with a core of  $10\ \mu\text{m}$  diameter and a cladding of an  $80\ \mu\text{m}$  overall diameter.

In Figs. 5 and 6 the results obtained for a  $20\ \mu\text{m}$  strain are presented. The splitting of laser electric field distribution can be observed in Fig. 6.

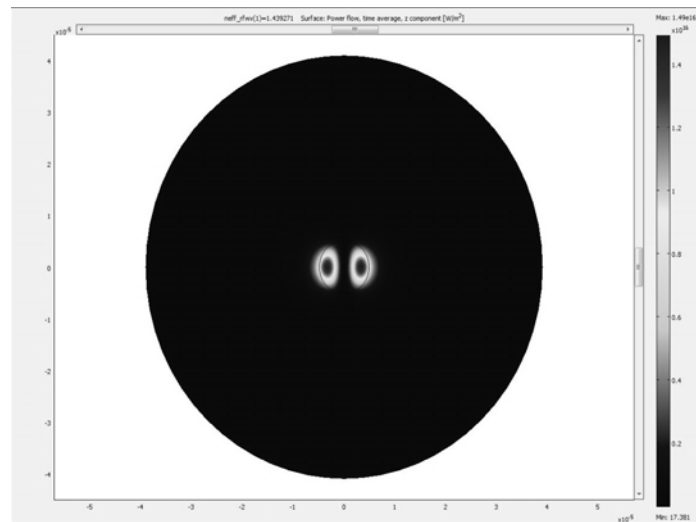


Fig. 5 – The numerical simulated time averaged laser power flow across the transverse section of a singlemode optical fiber with a core of  $8.82\ \mu\text{m}$  and  $11.33\ \mu\text{m}$  axes and a cladding of  $70.59\ \mu\text{m}$  and  $90.67\ \mu\text{m}$  axes.

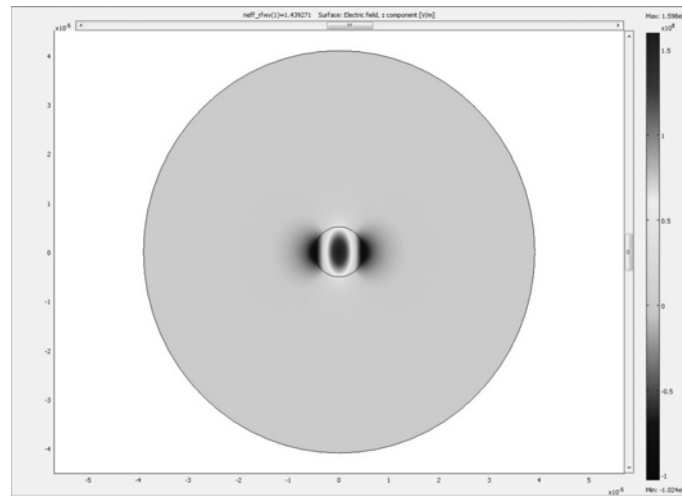


Fig. 6 – The numerical simulated time averaged laser electric field distribution into the transverse section of a singlemode optical fiber with a core of 8.82  $\mu\text{m}$  and 11.33  $\mu\text{m}$  axes and a cladding of 70.59  $\mu\text{m}$  and 90.67  $\mu\text{m}$  axes.

In Fig. 7 a diagram represents the variation with strain of maxim laser field power flow, maximum ( $E_{\text{max}}$ ) and minimum ( $E_{\text{min}}$ ) values of laser electric field. The continuous decrease of laser field parameters with the strain can be observed.

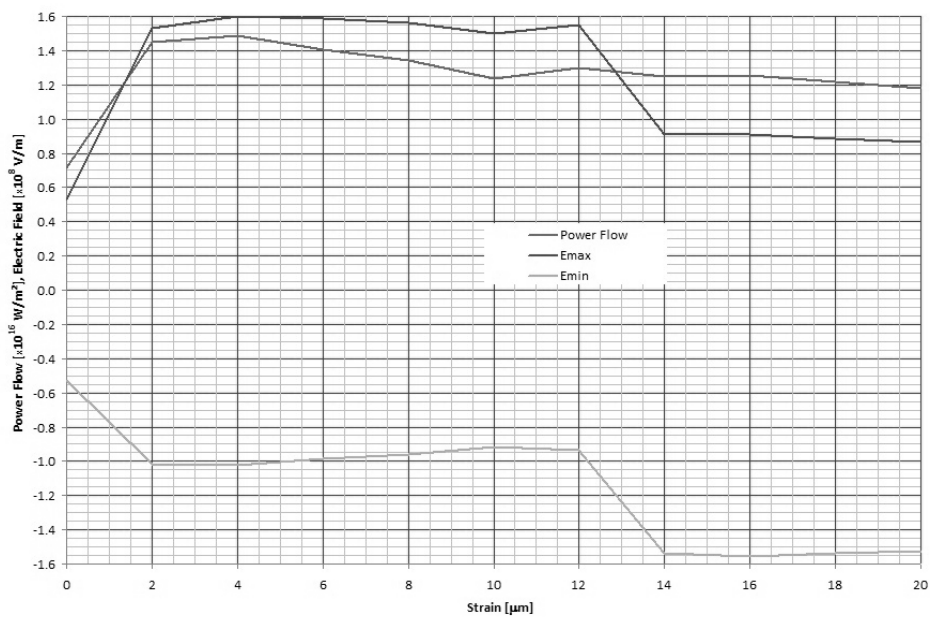


Fig. 7 – Variations with strain [ $\mu\text{m}$ ] of maxim laser field power flow, maximum ( $E_{\text{max}}$ ) and minimum ( $E_{\text{min}}$ ) values of laser electric field.

#### 4. CONCLUSIONS

The presented preliminary results in numerical simulation of optic fibre and laser fibre bending sensitivity lead to the conclusion that further developments are possible.

#### REFERENCES

1. G. Sorbello, S. Taccheo, P. Laporta, *Numerical modeling and experimental investigation of double-cladding erbium–ytterbium-doped fiber amplifiers*, *Optical Quantum Electron.*, **33**, 599–619 (2001).
2. E. Yahel, A. Hardy, *Modeling high-power Er–Yb codoped fiber lasers*, *J. Lightw. Technol.*, **21**, 9, 2044–2052 (2003).
3. E. Yahel, A. Hardy, *Modeling and optimization of short Er–Yb codoped fiber lasers*, *IEEE J. Quantum Electron.*, **39**, **11**, 1444–1451 (2003).
4. I. Lăncrăjan, S. Micloș, D. Savastru, *Numerical simulation of a DFB-fiber laser sensor (I)*, *J. Optoelectron. Adv. Mater.* **12**, 8, 1636–1645 (2010).